

Phase Behavior of Blends of Linear and Branched Polyethylenes in the Molten and Solid States by Small-Angle Neutron Scattering

R. G. Alamo,[†] J. D. Londono,[‡] L. Mandelkern,[†] F. C. Stehling,[§] and G. D. Wignall^{*‡}

Institute of Molecular Biophysics, Department of Chemistry, Florida State University, Tallahassee, Florida 32306-3015, Oak Ridge National Laboratory, Oak Ridge, Tennessee 37831-6393, and Plastics Technology Division, Exxon Chemical Company, Baytown, Texas 77520

*Received August 27, 1993; Revised Manuscript Received November 1, 1993**

ABSTRACT: The state of mixing in blends of high-density polyethylene (HDPE) and low-density polyethylene (LDPE) in the liquid and solid state has been examined by small-angle neutron scattering (SANS) in conjunction with deuterium labeling. In the melt, SANS results indicate that HDPE/LDPE mixtures form a single-phase solution for all concentrations, including blends containing high volume fractions ($\phi > 0.5$) of branched polymer, for which multiphase melts have previously¹⁻³ been suggested. Proper accounting for isotope effects is essential to avoid artifacts, because the H/D interaction parameter is sufficiently large ($\chi_{HD} \sim 4 \times 10^{-4}$) to cause phase separation in the amorphous state for molecular weights (MW) $> 150\,000$. In the solid state, after slow cooling from the melt (~ 0.75 °C/min), the HDPE/LDPE system shows extensive segregation into separate domains ~ 100 – 300 Å in size. Both the shape and magnitude of the absolute scattering cross section are consistent with the conclusion that the components are extensively segregated into separate lamellae. Two-peak melting curves obtained for such mixtures support the SANS interpretation, and the segregation of components in the solid state is therefore a consequence of crystallization mechanisms rather than incompatibility in the liquid state.

Introduction

Polyethylene is produced in many forms, each of which is partially crystalline with significantly different properties resulting from variations in structure. The melting temperatures of the different polyethylenes depend on both the molecular constitution and crystalline conditions. High-density polyethylene (HDPE) is the most crystalline with a (peak) melting temperature of typically 130 °C $< T_m < 135$ °C (depending on the thermal history), and because the chains contain very little branching, the density is quite high (0.95 – 0.97 g/cm³). Low-density polyethylene (LDPE), made by the free-radical-initiated polymerization of ethylene, contains some short-chain branches (principally butyl and ethyl branches, formed through intramolecular hydrogen-transfer reactions) as well as a few long-chain branches (formed through intermolecular hydrogen-transfer reactions between "live" polymer chains and previously formed "dead" polymer chains). It has a melting point of typically 108 °C $< T_m < 115$ °C and a density range of 0.91 – 0.94 g/cm³. Linear low-density polyethylene (LLDPE) is produced by copolymerizing ethylene with an α -olefin such as butene, hexene, or octene. The comonomer reduces the crystallinity of the linear polymer, making it more flexible while retaining its strength. The structure of the LLDPE is similar to the LDPE but with a homogeneous side branch length and no long-chain branches. LLDPE has a density range comparable to LDPE but with a melting point intermediate between HDPE and LDPE ($T_m \sim 125$ °C).

The properties of the individual species can be altered in a significant way by mixing the components, and blends

of HDPE, LDPE, and LLDPE have attained widespread commercial applications, as, for example, in LLDPE/LDPE blends which combine a high toughness of LLDPE with the good melt processability of LDPE. However, understanding of the mechanical and melt-flow properties of such blends is handicapped by the absence of a consensus in understanding at the most fundamental level, i.e., the degree of mixing of the components, in both the melt and solid states. For example, widely different views have been expressed in the literature ranging from liquid–liquid phase segregation¹⁻³ to complete homogeneity in the melt^{4,5} for HDPE/LDPE mixtures.

X-ray cloud-point measurements are insensitive to these alternatives because of the very small electron density contrast between the components. However, small-angle neutron scattering (SANS) can in principle supply such information via the strong contrast achieved by deuterating one of the components. There are large differences, in both the shape and absolute magnitude of the scattering from homogeneous⁶ and phase-separated⁷ systems. In the former case, the SANS technique permits the measurements of Flory–Huggins (FH) interaction parameters (χ) and molecular dimensions (radius of gyration, R_g) at various temperatures. Such experiments were attempted in the 1980s and were interpreted in terms of miscibility for HDPE/LDPE⁴ and HDPE/LLDPE⁸ in the melt. However, most of these data were never published, due to some puzzling features of the analysis that could not be explained at that time or because of uncertainties about the magnitude of the H/D isotope effect. For example, SANS experiments⁹ on 50/50 mixtures of HDPE/LDPE indicated that the components were compatible in the melt when only part of the HDPE was deuterium-labeled. However, if all of the HDPE was deuterated, the system apparently phase separated.

As a result of subsequent advances in the understanding of polymer isotope effects in general^{16,7} and polyethylenes in particular,¹⁰ we believe that a solution of this long-standing problem has now been accomplished. Due to

[†] Florida State University.

[‡] Oak Ridge National Laboratory (managed by Martin Marietta Energy Systems, Inc., under Contract DE-AC05-84OR21400 for the U.S. Department of Energy).

[§] Exxon Chemical Co.

* Abstract published in *Advance ACS Abstracts*, December 15, 1993.

Table 1. Molecular Weights of Homopolymer Components of Blends (All Components Are Protonated Unless Otherwise Stated)

			branches/100 backbone carbon	
	$10^3 M_w$	M_w/M_n	long ^d	short ^c
Series A				
HDPE-1D	201 ^a	3.4	0	0
LDPE-1	110 ^c	5.1	0.15	1.2
LDPE-2	212 ^c	17.2	0.25	1.6
Series B				
HDPE-2D	101 ^a	2.9	0	0
HDPE-1	149 ^b	3.6	0	0
LDPE-3	136 ^c	11.0	0.28	1.31

^a For HDPE-D the MW was calculated as if it contained H atoms rather than D atoms. The degree of polymerization can be calculated for both species by dividing MW by 28. ^b For HDPE, MWs were obtained from standard size-exclusion chromatography (SEC). ^c For LDPE, MWs were obtained using a SEC-intrinsic viscosity procedure as described previously.^{29,30} ^d Branches containing >8 carbon atoms (via NMR). ^e Branches containing ≤8 carbon atoms (via NMR).

recent measurements¹⁰ of the isotopic interaction parameter (χ_{HD}) between labeled (C_2D_4) and unlabeled (C_2H_4) segments, it is clear that the degree of polymerization (N) in the initial experiments^{4,9} was sufficiently large to exceed the critical condition for demixing ($N\chi_{HD} = 2$). Thus, phase segregation at higher labeling levels was caused by isotope effects, rather than incompatibility of the components. In this paper we report data from a series of blends of HDPE and LDPE with lower molecular weight (and hence lower N). The product $N\chi_{HD} < 2$ and SANS experiments indicate homogeneity in the melt for all compositions. The components are shown to demix on slow cooling to the solid state due to differential crystallization effects, whereby the higher melting component crystallizes first and the degree of segregation is a function of the cooling rate. This research is relevant to determining phase structures, to interpreting observed property changes on mixing, and to guiding strategies to improve blend properties.

Sample Preparation and Characterization

Two sets of samples were prepared from the materials shown in Table 1. The initial^{4,9} experiments were performed with the Series A samples, some of which are now understood to have phase separated in the melt due to isotope effects. This series includes LDPEs with different weight- or number-averaged molecular weights (M_w or M_n), whose phase behavior may be used to test the hypothesis of isotope-driven phase segregation. Subsequently, a further set of samples (Series B) was prepared with lower MW, thus avoiding the isotopic phase-separation effects. Table 1 shows the molecular weights of the blend components, which were chosen to simulate the behavior of commercial systems. Thus, the polydispersities, as measured by gel permeation chromatography (GPC), were quite high, with M_w/M_n in the range 3–5 for the HDPE molecules. For the LDPE samples, values of M_w/M_n were in the range 5–17, though the phase stability was independent of polydispersity to a very good approximation.

For Series A, weighed amounts of the deuterated (d-4) linear polymer HDPE-1D (98% D; Merck Lot 300-F) were mixed with branched polymer (LDPE-1 or LDPE-2) as follows: Weighed amounts of both polymers (total quantity ~1 g) were dissolved in 200 cm³ of trichlorobenzene containing 0.2 g of 4-methyl-2,6-di-*tert*-butylphenol (BHT) at 160 °C with stirring under nitrogen for 2 h. The solution was then poured into 400 cm³ of methanol at room temperature. The precipitated polymer was dried in a vacuum oven (~60 °C) to constant weight. Total amounts of 0.1% BHT and 0.1% distearyl-pentaerythritol diphosphate stabilizer were added by evaporating an acetone solution containing these additives onto the powdered precipitate. The samples were molded into disks ~1.5-mm thick in a hydraulic manual press, for 5 min at 176 °C between hot platens, followed by rapid cooling

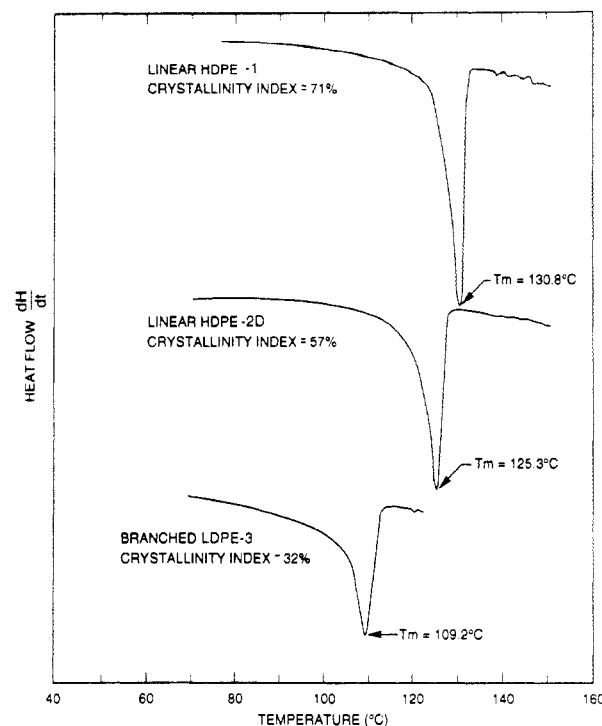


Figure 1. Initial DSC scans (10 °C/min) for linear and branched PE homopolymers after quenching into ice-water.

between cold platens. The average cooling rate between 150 and 80 °C was 300 °C/min.

For Series B the mixtures were prepared by dissolving deuterated polymer (HDPE-2D; Merck Isotopes MD-775) with either linear (HDPE-1) or branched (LDPE-3) protonated polymer (total weight ~300 mg) in 125 mL of *o*-dichlorobenzene at 177 °C and stirred for 15 min. The solution was rapidly quenched into 2.2 L of chilled (~-60 °C) methanol, and after filtering, the crystals were dried overnight in a vacuum oven at 60 °C. Disks ~1-mm thick were obtained via compression molding at 190 °C and quenching into ice-water. The thermal behavior was studied via differential scanning calorimetry (DSC) for both sample series, with similar results. The pure components gave single endotherms in all cases (Figure 1), though the branched polymer (LDPE-3 in Figure 1) melts over a wider range and has a lower crystallinity and (peak) melting temperature ($T_m \sim 109$ °C) than the linear polymers. These gave sharper endotherms, peaked at higher temperatures, though deuterated polyethylene (HDPE-2D in Figure 1) melts at a lower temperature ($T_m \approx 125$ °C) than its protonated counterpart ($T_m \approx 131$ °C).

Small-Angle Neutron Scattering: Data Collection

The data were collected on the W. C. Koehler 30-m SANS facility¹¹ at the Oak Ridge National Laboratory (ORNL) via a 64 × 64 cm² area detector with cell (element) size ~1 cm² and a neutron wavelength (λ) 4.75 Å. The detector was placed at sample-detector distances in the range 14–19 m, and the data were corrected for instrumental backgrounds and detector efficiency on a cell-by-cell basis, prior to radial averaging to give a Q -range of $0.003 < Q = 4\pi\lambda^{-1} \sin \theta < 0.04 \text{ Å}^{-1}$, where 2θ is the angle of scatter. The sample cross sections were obtained by subtracting the intensities of the corresponding sample cells with quartz windows, which formed only a minor correction (<5%) to the sample data. The net intensities were converted to an absolute ($\pm 3\%$) differential cross section per unit sample volume [$d\Sigma/d\Omega(Q)$ in units of cm⁻¹] by comparison with precalibrated secondary standards, based on the measurement of beam flux, vanadium incoherent cross section, the scattering from water, and other reference materials.¹² The efficiency calibration was based on the scattering from light water, and this led to angle-independent scattering for vanadium, H-polymer

blanks, and water samples of different thickness in the range 1–10 mm. The cross section of various fully labeled (PED) and unlabeled (PEH) linear and branched blanks was also measured as a basis for subtracting the coherent and incoherent backgrounds.¹³ The former arises principally from void scattering at low Q and is negligible for $Q > 0.01 \text{ \AA}^{-1}$. The latter is a flat background $\sim 0.1\text{--}0.7 \text{ cm}^{-1}$, due to the H^1 incoherent cross section ($\sigma \sim 80 \times 10^{-24} \text{ cm}^2$) and may be subtracted via empirical methods.¹³

At room temperature, the transmission of the sample was measured in a separate experiment by collimating the beam with slits (irises) $\sim 1 \text{ cm}$ in diameter, separated by a distance $\sim 7.5 \text{ m}$. A strongly scattering sample, porous carbon, was placed at the sample position to spread the beam over the whole detector, with a sample–detector distance $\sim 14 \text{ m}$. Without the carbon in position, the beam would either be blocked by the beam stop or concentrated in a few detector cells, with the possibility of saturating or damaging the detector. The total count summed over the whole detector ($>10^5$) was recorded in a time period $\sim 1 \text{ min}$, and the polymer sample was then placed over the source slit, thus attenuating the beam. The count was repeated over the same time interval, and the transmission is given by the ratio of the two counts after minor corrections ($<0.1\%$) for the background due to electronic noise, cosmic rays, etc. In this geometry no scattering from the sample at Q values $> 10^{-3} \text{ \AA}^{-1}$ can enter the second iris and be rescattered by the porous carbon to be counted by the detector.

Because the H^1 incoherent cross section is temperature dependent, a variation on this method was used to measure the transmission at the particular temperature of each measurement, by placing the (heated) polymer over the sample slit. In this geometry, the scattering from the sample can also be recorded by the detector, and thus a correction must be made for this component. However, the cross section of the porous carbon is 2–3 orders of magnitude larger than the sample signal (which is itself attenuated by the porous carbon), and thus the adjustment for this effect is small ($<2\%$). Typically, the transmission of a 1-mm-thick sample of a 50/50 blend changed by $<1\%$ between room temperature at 200°C , because the increasing incoherent cross section of H^1 is offset by the decreasing density of the polymer.

Small-Angle Neutron Scattering: Data Analysis

The initial applications of SANS to investigate polymer compatibility were based on an extension to polymer blends of the Zimm analysis,¹⁴ originally developed for light and small-angle X-ray scattering (SAXS) to give R_g , M_w , and the second virial coefficient A_2 . In principle, the Zimm analysis is limited to the regime where one of the species is dilute, though it has been extended^{14–16} to concentrated homogeneous mixtures to give the FH interaction parameter (χ), which is related to A_2 in dilute systems.¹⁴ For a blend of two polymer species (A and S), one of which (A) is deuterium labeled, the coherent cross section (after subtracting the incoherent background) is given^{6,7} by

$$\frac{d\Sigma}{d\Omega}(Q) = V^{-1}(a_H - a_D)^2 S(Q) \quad (1)$$

where a_D is the scattering length of the labeled repeat unit (segment) of the A species (HDPE-D in this research), and a_H is the scattering length of the unlabeled S species (LDPE-H). The segment (C_2H_4) volume (V) is assumed to be the same for both species in the melt, which is a reasonable assumption for blends of HDPE and LDPE in view of the small number of branches. An important

achievement in elucidating blend thermodynamics was the mean-field random-phase approximation (RPA)¹⁶ to derive the structure factor $S(Q)$. Assuming that the polymer constituents can be treated as ideal (Gaussian) coils, unperturbed by the weak interactions between monomers, $S(Q)$ is given by^{14–17}

$$S^{-1}(Q) = [\phi_A N_A P_A(QR_{gA})]^{-1} + [(1 - \phi_A) N_S P_S(QR_{gS})]^{-1} - 2\chi \quad (2)$$

where ϕ_A is the volume fraction of the A species and R_{gA} , R_{gS} , N_A , and N_S are the radii of gyration and polymerization indices of the two species, with intrachain functions $P_A(Q)$ and $P_S(Q)$ represented by Gaussian coils.¹⁶ In the dilute ($\phi \rightarrow 0$) limit, eq 2 reduces to the traditional Zimm equation, used extensively in early SANS studies of polymer mixtures.¹⁴ At small scattering wavevectors (Q), eqs 1 and 2 reduce to the well-known Ornstein–Zernike (OZ) form^{16,17}

$$\frac{d\Sigma}{d\Omega}(Q) = \frac{d\Sigma}{d\Omega}(0)/(1 + Q^2\xi^2) \quad (3)$$

$$\frac{d\Sigma}{d\Omega}(0) = \frac{V^{-1}(a_H - a_D)^2}{(\phi_A N_A + \phi_S N_S - 2\chi)} \quad (4)$$

where ξ is the composition fluctuation correlation length. In this work the SANS data are analyzed both by RPA fits (nonlinear least-squares regression to eqs 1 and 2) and also by OZ fits (linear regression to eq 3 at small Q). The latter methodology provides a complementary mode of analysis, independent of the assumptions made about $P(Q)$ in the RPA. Identical conclusions concerning the phase stability are given by both approaches, which extrapolate to the same value of $d\Sigma/d\Omega(0)$, from which the value of χ is calculated.

Equations 1 and 2 were originally derived for monodisperse systems, though the extension to polydisperse blends has been given by Boué et al.,¹⁸ whose showed that N_A and N_S are replaced by their weight-averaged values. R_{gA} and R_{gS} are weighted by the ratio of the z and weight averages of the distribution.¹⁸ The molecular polydispersity (Table 1) prevents a precise determination of the reduction of the chain dimensions caused by branching but does not affect the determination of χ or conclusions concerning phase stability (see below).

These equations contain only one interaction parameter and are therefore limited to two possible cases: first, where isotope effects may be neglected and the interspecies interaction parameter (χ_{HS} or χ_{DS}) is much greater than χ_{HD} ; alternatively, the isotopic interaction may dominate interspecies interactions ($\chi_{HD} \gg \chi_{HA}$, $\chi_{HD} \gg \chi_{DS}$), and we believe that this is a good approximation for HDPE/LDPE mixtures in view of the basic similarity of the chains and the small number of branches involved. Crist and co-workers^{19,20} have studied blends of hydrogenated polybutadienes, which are structurally analogous to ethylene/butene-1 copolymers. They have estimated an interspecies interaction parameter between branched and linear molecules as $\chi = CY_{Br}^2$ ($T = 150^\circ\text{C}$), where Y_{Br} is the fraction of branched C_4H_8 units and C is an experimentally determined constant. Values of $C = 0.014$ and 0.022 have been determined via SANS¹⁹ and morphological observations,²⁰ respectively. Assuming typically 1.5 branches per 100 C atoms for LDPE (Table 1), this leads to $Y_{Br} \approx 0.058$ and $\chi \sim (0.45\text{--}0.75) \times 10^{-4}$ for the C_4H_8 unit [or $\chi \sim (0.23\text{--}0.38) \times 10^{-4}$ for the C_2H_4 repeat unit used in this paper]. Thus, for the blends studied in this work, the interspecies interaction parameter may be expected to be only a small perturbation on the isotopic interaction ($\chi_{HD} \approx 4 \times 10^{-4}$). Furthermore, Rhee and Crist have demon-

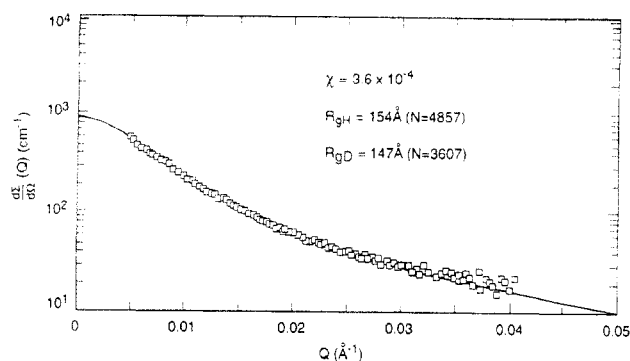


Figure 2. Fit to the random-phase approximation for a blend of branched LDPE ($\phi_H = 0.53$) and deuterated linear HDPE ($\phi_D = 0.47$) at 155 °C.

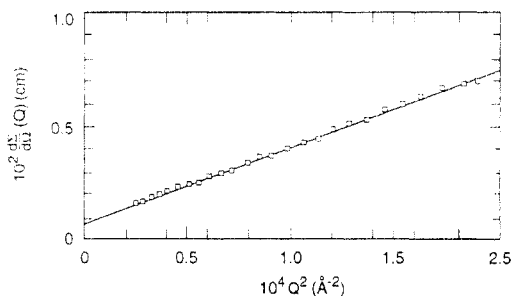


Figure 3. Ornstein-Zernike plot of SANS from a blend of branched LDPE ($\phi_H = 0.53$) and deuterated linear HDPE at ($\phi_D = 0.47$) at 155 °C.

strated²¹ that the interaction parameter is minimized when the less branched component is labeled and a similar "switching effect" has been observed by Graessley et al.²² It will be seen that the (total) interaction parameters measured in HDPE-D/LDPE blends (where the deuterated component is unbranched) are virtually identical to the (isotopic) interaction measured in linear/linear systems,¹⁰ thus confirming this hypothesis. With the benefit of hindsight, the phase behavior in the melt should therefore be dominated by isotope effects, as originally observed.^{4,9} Equations 1–4 may therefore be applied to HDPE/LDPE blends with a single interaction parameter (χ_{HD}) to a good approximation.

Results and Discussion

Figure 2 shows the scattering cross section $d\Sigma/d\Omega$ vs Q for a "50/50" (wt %) blend of deuterated HDPE-2D ($\phi_D = 0.467$, $M_w = 101 \times 10^3$) and protonated LDPE-3 ($\phi_H = 0.533$, $M_w = 136 \times 10^3$) at 155 °C (series B in Table 1). After allowing the sample to equilibrate for ~ 10 min, the data were collected over time periods ~ 1 h. The fit to the RPA (eqs 1 and 2) is excellent and leads to a value of the total interaction parameter, $\chi \approx (3.6 \pm 0.5) \times 10^{-4}$. This is close to the isotopic interaction parameter measured¹⁰ in linear/linear blends [$\chi_{HD} = (3.9 \pm 0.3) \times 10^{-4}$] at the same temperature. The $Q = 0$ intercept, $d\Sigma/d\Omega(0) \sim 900 \text{ cm}^{-1}$, is approximately 3 times the value expected for $\chi = 0$, and this ratio gives a measure of the signal-to-noise of the determination. Figure 3 shows an Ornstein-Zernike plot ($d\Sigma/d\Omega^{-1}$ vs Q^2) of the same data, which has a positive intercept (after linear extrapolation to $Q = 0$), and is characteristic of homogeneous (one-phase) systems. The DSC thermograms (Figure 4a) of the 50/50 mixture show only one peak at 121.1 °C, after the sample was quenched into ice-water. These observations are consistent with the previous conclusion based solely on the study of the crystalline state that the HDPE/LDPE system is homogeneous near the center of the phase diagram.^{1–3}

Figures 5 and 6 give the SANS data for a mixture

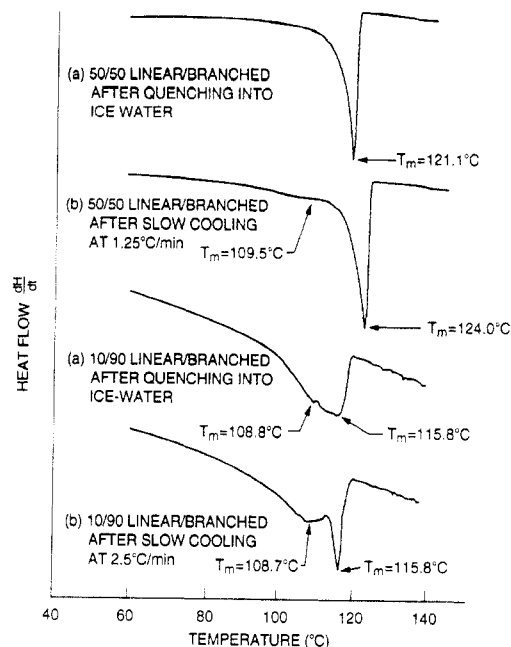


Figure 4. DSC thermograms (10 °C/min) for mixtures and linear (PED) and branched polyethylenes after (a) quenching SANS samples into ice-water and (b) slow cooling from the melt.

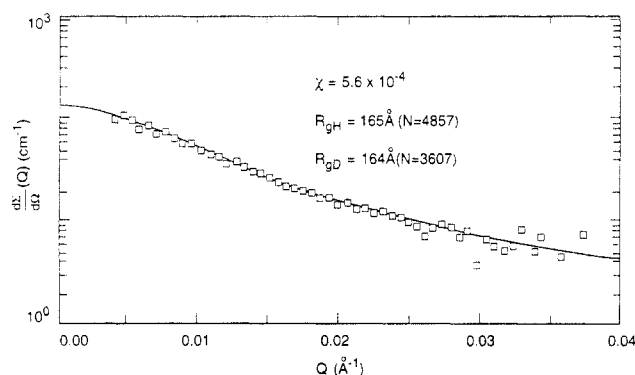


Figure 5. Fit to the random-phase approximation for a blend of branched LDPE ($\phi_H = 0.91$) and deuterated linear HDPE ($\phi_D = 0.09$) at 143 °C.

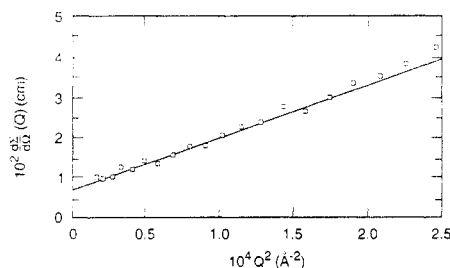


Figure 6. Ornstein-Zernike plot of SANS from a blend of branched LDPE ($\phi_H = 0.91$) and linear HDPE ($\phi_D = 0.09$) at 143 °C.

containing a higher content ($\phi_H = 0.91$) of the branched polymer (LDPE-3) and a low concentration of linear HDPE-2D ($\phi_D = 0.09$). The RPA fit (Figure 5) and OZ plot (Figure 6) are both characteristic of a homogeneous blend. This result and similar data at $\phi_D = 0.207$ provide direct evidence of the state of mixing in the melt and show that HDPE/LDPE blends with high concentrations of branched polymer consist of a single phase. They contradict the hypothesis of a two-phase melt,^{1–3} based on indirect measurements of the solid state.

The value of $\chi = (5.6 \pm 0.6) \times 10^{-4}$ is close to the isotopic interaction parameter measured at the same temperature ($T = 143$ °C) in linear/linear mixtures.¹⁰ This value is higher than the 50/50 blend (Figure 2) and thus reproduces

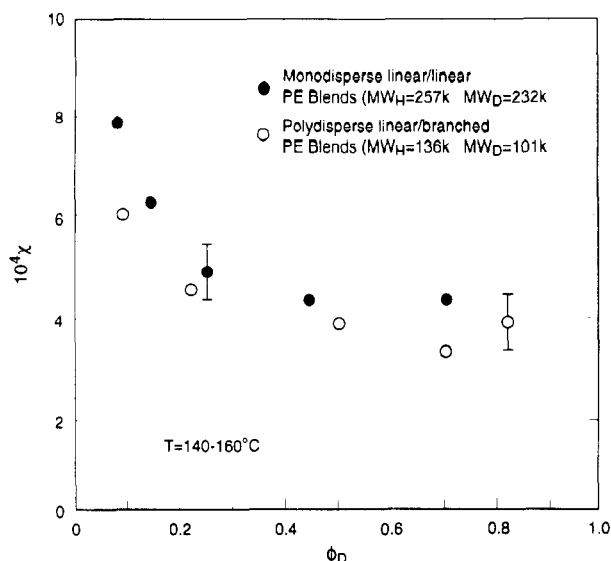


Figure 7. Total interaction parameter (χ) measured in branched-linear blends compared to χ_{HD} measured in linear-linear systems.

the concentration dependence of χ_{HD} in linear/linear blends.¹⁰ Figure 7 compares the total interaction parameter measured in polydisperse HDPE-D/LDPE blends (this work) with the isotopic interaction parameter (χ_{HD}) measured in monodisperse ($M_w/M_n \sim 1.2$) linear/linear mixtures.¹⁰ The agreement is very good, thus confirming that the interspecies χ is only a small perturbation on the isotopic interaction and that polydispersity effects do not affect our conclusions concerning phase stability. The close agreement between the interaction parameters measured in HDPE-D/LDPE and χ_{HD} in linear/linear blends indicates that the use of the RPA formalism is reasonable. As a cross-check on the validity of this methodology in cases where one of the chains is branched, the RPA was reformulated to fit the data using the form factors of a linear chain (Debye coil) and an n -arm star.²³ Allowing the number of arms (n) to float as a fitting parameter for the branched component produced a change in χ of less than 5%.

The R_g 's (e.g., Figures 2 and 5) of the branched chains were smaller than for linear chains of equivalent MW, though the polydispersity of the components (Table 1), precluded a precise measurement of the differences. Such determinations using more monodisperse molecules would be worthwhile, though the current uncertainties in the dimensions of branched molecules do not affect the conclusions concerning the homogeneity of the melt. In view of the excellent linearity of the OZ plots (Figures 3 and 6), the data can be equally well extrapolated to $Q = 0$ via linear regression of the OZ formalism (eq 3) or nonlinear least-squares fitting to the RPA (eq 1 and 2). Either method gives the same value of $d\Sigma/d\Omega(0)$, from which the χ parameter is obtained, and thus the conclusions are independent of the mode of data analysis.

Figure 8 shows SANS data at 150 °C for a linear/linear blend (HDPE-2D/HDPE-1) with virtually the same concentrations of deuterated and protonated components ($\phi_D = 0.106$; $\phi_H = 0.894$) as the branched/linear combination shown in Figure 5. Both the fitted interaction parameter [$\chi = (4.7 \pm 0.4) \times 10^{-4}$] and intensities are virtually the same as for the HDPE/LDPE blend at a similar concentration (Figure 5). The linear/linear blend is homogeneous by definition, and the close correspondence with the branched/linear data confirms that the latter system is also homogeneous in the melt. Similar data at other compositions ($\phi_D = 0.207, 0.671, 0.78$) lead to the same conclusions derived from Figures 2 and 5. Thus, blends

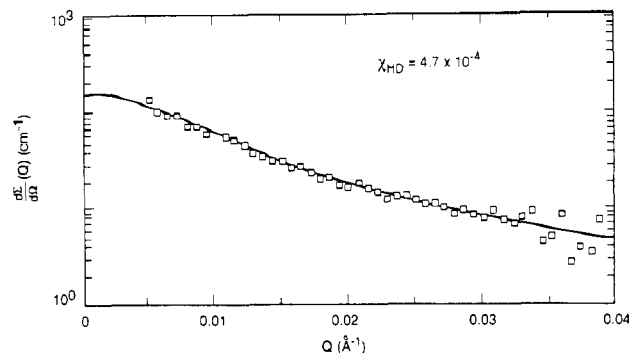


Figure 8. Fit to the random phase approximation for a blend of linear protonated ($\phi_H = 0.89$) and deuterated ($\phi_D = 0.11$) HDPEs at 150 °C.

of HDPE/LDPE molecules with MWs indicated in Table 1 (series B) are homogeneous in the melt over the complete concentration range.

In view of the different conclusions drawn from solid-state measurements¹⁻³ and those reached via SANS from the melt for low concentrations of linear polymer (particularly for $\phi_D = 0.09$ and $\phi_D = 0.207$), we have performed DSC on selected SANS samples after cooling from the melt. Figure 4 shows such data on both quenched and slowly cooled samples. For the 10/90 blend containing predominantly branched material ($\phi_H = 0.91$; $\phi_D = 0.09$), two endothermic peaks are clearly resolved in the slowly crystallized material, though for the quenched blend a broad melting curve is observed with no obvious separation into two peaks. However, it should be pointed out that in these mixtures, the linear component is deuterated and hence has a melting point ~ 6 °C lower than its protonated equivalent. Thus the thermodynamic driving force for peak separation is less than in previous studies, where two endotherms were observed¹⁻³ in protonated blends containing a high content of branched material. Complementary DSC measurements on blends where both components are protonated (e.g., "10/90" mixtures of HDPE-1/LDPE-3) confirm that two endotherms are clearly observed after quenching, though the SANS results make it quite evident that the blends are homogeneous in the molten state.

These results emphasize the inherent uncertainties in attempting to deduce the (amorphous) melt structure from the melting behavior and morphology of the solid (crystalline) state. Only under special circumstances (e.g., where the size scale of the solid-state morphology increases with the annealing time in the melt²⁰) is there a one-to-one correspondence between the phase separation observed in the melt and solid state. For HDPE/LDPE blends, the narrow melt endotherm of the linear polymer makes it easier to detect small amounts of such material in a predominantly branched matrix after they have each crystallized separately on cooling from the homogeneous melt (Figure 4b). Conversely, the broad melt endotherm and low crystallinity (Figure 1) of the branched material make it difficult to detect concentrations of less than 50% of this component, even after slow cooling from the melt (Figure 4b). Furthermore, for a given molecular weight, the diffusion coefficients of branched molecules are much lower than their linear counterparts and this inhibits the possibility of forming separate domains of branched polymer in a predominantly linear matrix. Thus, blends with low concentrations ($\phi < 0.5$) of branched materials naturally give rise to single endotherms on cooling, whereas, for $\phi > 0.5$, two-peaked endotherms are observed. However, the SANS results reported here make it evident that such behavior arises from crystallization effects rather than a multiphase melt.

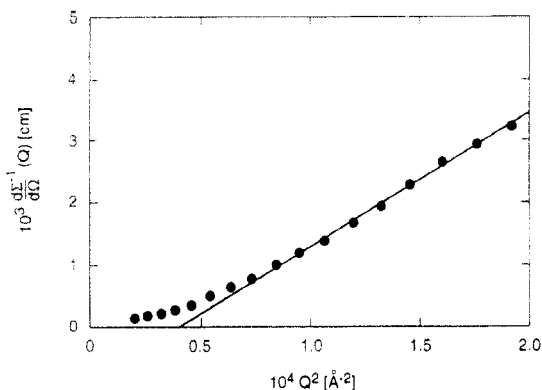


Figure 9. OZ plot for a 50/50 mixture of linear PED (MW = 201×10^3) and branched PEH (MW = 212×10^3) at 165 °C.

It might be argued in support of the hypothesis of a biphasic melt¹⁻³ that segregation occurs on such a large length scale that any scattering due to the phase structure would be at Q values lower than the SANS resolution limit ($Q \sim 2\pi/0.003 \sim 2000 \text{ Å}$). In such a case, the observed scattering might arise from the mixed phase within the phase-separated domains. However, this explanation requires a remarkable series of coincidences to produce the observed intensities. First, one has to demonstrate why domains of less than 2000 Å in size are ruled out, and, second, the mixed domains must appear in just sufficient quantities and compositions to reproduce the intensity expected from a homogeneous melt. We believe that it is highly unlikely that the close similarity of the SANS data (e.g., Figures 2 and 5) and resulting χ parameters (e.g., Figure 7) could occur if the samples were phase separated for $\phi_D < 0.5$ and homogeneous for $\phi_D > 0.5$. There is no suggestion of a discontinuity at $\phi_D = 0.5$ (Figure 7), and the simplest explanation is that the melt is homogeneous over the whole concentration range.

Bates and co-workers⁷ demonstrated that phase separation on the micron length scale produces strong excess SANS scattering in the Q range used in this work. Furthermore, the extreme sensitivity of SANS to phase separation in polyolefin melts can be further illustrated via experiments using higher molecular weight components (series A). Figure 9 shows an OZ plot of data from a mixture of labeled HDPE-1D ($\phi_D = 0.467$; $M_w = 201 \times 10^3$) and LDPE-2 ($\phi_H = 0.533$; $M_w = 212 \times 10^3$) at 165 °C. Assuming an interaction parameter ($\chi_{HD} \approx 4 \times 10^{-4}$), the product ($N\chi_{HD} \sim 3$) exceeds the value for phase separation and the OZ plot extrapolates to a negative intercept. When the data are plotted in a form appropriate for two-phase systems (e.g., $d\Sigma/d\Omega^{-1/2}$ vs Q^2 as proposed by Debye et al.²⁴), the cross section ($\sim 10^4 \text{ cm}^{-1}$ at $Q = 0$) is over an order of magnitude higher than that for one-phase systems (e.g., Figure 2). For lower MW samples, e.g., 50/50 blends of HDPE-1D ($\phi_D = 0.467$; $M_w = 201 \times 10^3$) and LDPE-1 ($\phi_H = 0.523$; $M_w = 110 \times 10^3$), the isotope effect is barely sufficient to induce phase segregation and the intercept is just slightly negative (Figure 10).

The above experiments indicate that isotope effects constitute the main thermodynamic driving force for segregation and that protonated HDPE/LDPE blends are homogeneous in the melt. However, components may separate on slow cooling due to the difference in crystallization mechanisms. Figure 11 shows a Debye-Bueche²⁴ (DB) plot of the data for the 50/50 blend shown in Figure 2, after cooling from the melt at 0.75 °C/min. The extrapolated cross section [$d\Sigma/d\Omega(0) = 24.5 \times 10^3 \text{ cm}^{-1}$] is well over an order of magnitude higher than in the melt, indicating that the components have phase separated on

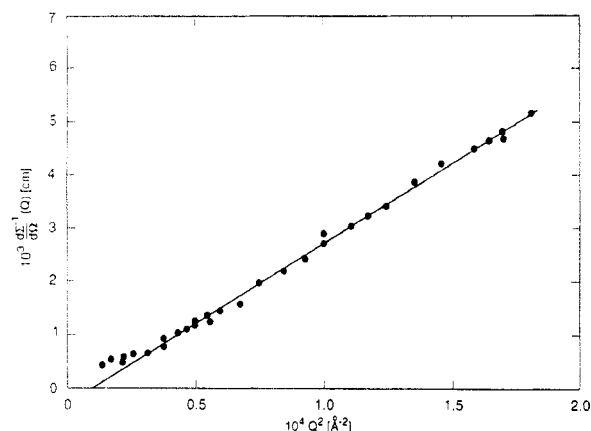


Figure 10. OZ plot for a 50/50 mixture of linear PED (MW = 201×10^3) and branched PEH (MW = 110×10^3) at 165 °C.

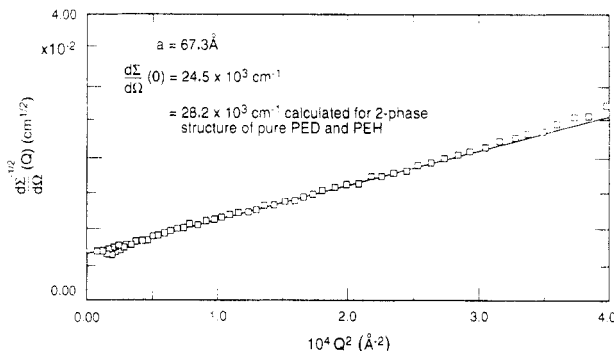


Figure 11. Debye-Bueche plot for phase-separated blend of deuterated HDPE and protonated LDPE slow cooled from the melt at 0.75 °C/min.

cooling. The plot is reasonably linear and the ($Q = 0$) cross section is given^{17,25} by

$$\frac{d\Sigma}{d\Omega}(0) = 8\pi a^3 \phi_1 \phi_2 [\text{SLD}(1) - \text{SLD}(2)]^2 \quad (5)$$

where the correlation length (a) is derived^{24,25} from the ratio of the slope/intercept of the DB plot, ϕ_1 and ϕ_2 are the volume fractions, and $\text{SLD}(1)$ and $\text{SLD}(2)$ are the scattering length densities of the two phases.²⁵ Assuming complete separation of the deuterated and protonated components (i.e., $\phi_1 = \phi_D$, $\phi_2 = \phi_H$), the calculated cross section is $28.2 \times 10^3 \text{ cm}^{-1}$, which is close to the experimental result. In view of the fact that the experiments are independently calibrated with no arbitrary fitting factors in the intensity scale, the agreement with the absolute cross sections calculated from the DB theory is excellent. As $Q \rightarrow \infty$, the cross section varies as Q^{-4} and this implies that the boundaries between the phases are sharp. The sizes of the domains may be estimated from the mean chord intercept lengths^{24,25} ($L_1 = a/\phi_1$, $L_2 = a/\phi_2$) and for $\phi_1 \approx \phi_2$; $L_1 \approx L_2 \approx 175 \text{ Å}$.

Figure 12 shows absolutely calibrated SAXS data for this sample collected on the ORNL 10-m SAXS camera, with pinhole collimation²⁶ and hence minimal instrumental smearing effects.²⁷ It is not unexpected that such a heterogeneous blend does not exhibit a clearly defined peak reflecting the lamellar period, as would be expected for example from slowly cooled HDPE. There are suggestions of "peaks" or modulations at $Q \sim 0.02$ and 0.055 Å^{-1} , which show up more clearly in the Lorentz-corrected plot ($Q^2 d\Sigma/d\Omega$ vs Q), though this is partly due to the fact that replotted data are constrained to pass through zero at $Q = 0$ (Figure 12b). The peak positions at $Q^* \sim 0.023$ and 0.055 Å^{-1} correspond to length scales of $D \approx 2\pi/Q^* \sim 275$ and 115 Å , which are of the same order as the average mean chord intercept length. It therefore seems reasonable

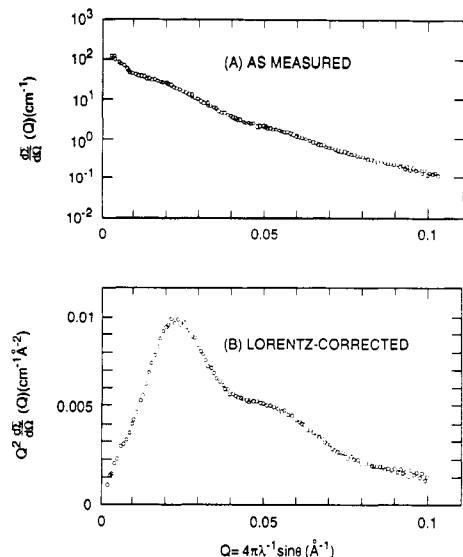


Figure 12. As measured and Lorentz-corrected SAXS cross sections of a 50/50 blend of branched (LDPE) and linear (HDPE) polyethylenes.

to associate the phase-separated domains with individual lamellae. We are exploring this hypothesis via further measurements over a wide range of concentration for samples crystallized in different ways (quenched, slow-cooled, etc.).

SANS studies are also being extended to HDPE/LLDPE blends in melt and solid states. The initial data obtained in the earlier studies⁹ also indicate homogeneity in the melt at $\phi \sim 0.5$, when isotope effects are properly accounted for. A similar conclusion was reached by Ree, Stein, and Lin.⁸ Slow cooling this blend produces samples with a much lower degree of segregation, which is consistent with a smaller difference in melting points and a single melting peak observed by DSC. We are also studying the time scale over which segregated blends homogenize on remelting.

Summary and Conclusions

The results described above make it quite evident that unlabeled HDPE/LDPE blends with $MW \sim (1-2) \times 10^5$ are homogeneous in the melt over the complete composition range, irrespective of the homogeneity of the parent crystalline state. This conclusion is contrary to that previously reported,¹⁻³ and the reason for this apparent discrepancy is that in the previous work attention was focused solely on the structure of the crystalline state. Admittedly, an initial heterogeneous melt will lead to a segregated crystalline state. However, it does not follow that the observation of a segregated crystalline state reflects a heterogeneous melt. Crystallization from a homogeneous melt of such species can easily lead to a segregated crystalline state as a consequence of the crystallization process and mechanism. The present work illustrates that a segregated crystalline state, as demonstrated by DSC and SANS, arises from a SANS-demonstrated homogeneous melt.

This research is relevant for evaluating the potential for recycling the different types of polyethylenes, which contribute approximately 50% of plastic wastes. Determining the degree of compatibility of the various components of polyolefin blends²⁸ in the melt and as a function

of the cooling rate has important implications for designing strategies for reprocessing such materials.

Acknowledgment. We are grateful to B. Crist (Northwestern University), D. J. Lohse (Exxon Research and Engineering Co.), and R. S. Stein (University of Massachusetts) for helpful discussions and for providing access to research in progress prior to publication. The SAXS measurements were performed by J. S. Lin and research at Oak Ridge National Laboratory was supported by the Division of Materials Sciences, U.S. Department of Energy under Contract No. DE-AC05-84OR21400 with Martin Marietta Energy Systems, Inc. The work at Florida State University was supported by the National Science Foundation Polymer Program (Grant DMR 89-14167), whose aid is gratefully acknowledged.

References and Notes

- Barham, P. J.; Hill, M. J.; Keller, A.; Rosney, C. C. A. *J. Mater. Sci. Lett.* **1988**, *7*, 1271.
- Hill, M. J.; Barham, P. J.; Keller, A.; Rosney, C. C. A. *Polymer* **1991**, *32*, 1384.
- Hill, M. J.; Barham, P. J.; Keller, A. *Polymer* **1992**, *33*, 2530.
- Stehling, F. C.; Wignall, G. D. *Polym. Prepr. (Am. Chem. Soc., Div. Polym. Chem.)* **1983**, *24*, 211.
- Hu, S. R.; Kyu, T.; Stein, R. S. *J. Polym. Sci., Polym. Phys. Ed.* **1987**, *25*, 71. Toshiro, K.; Stein, R. S.; Hsu, S. L. *Macromolecules* **1992**, *25*, 1801.
- Wignall, G. D.; Bates, F. S. *Makromol. Chem.* **1988**, *15*, 105. Bates, F. S.; Wignall, G. D.; Koehler, W. C. *Phys. Rev. Lett.* **1985**, *55*, 2425.
- Bates, F. S.; Dierker, S. B.; Wignall, G. D. *Macromolecules* **1986**, *19*, 1938; **1986**, *19*, 932.
- Ree, M.; Stein, R. S.; Lin, J. S., unpublished data (1986). Stein, R. S. NATO Workshop on Crystallization of Polymers, Mons, 1992.
- Stehling, F. C.; Wignall, G. D., unpublished data (1982).
- Londono, J. D.; Narten, A. H.; Wignall, G. D.; Honnell, K. G.; Hsieh, E. T.; Johnson, T. W.; Bates, F. S., submitted to *Macromolecules*.
- Koehler, W. C. *Physica (Utrecht)* **1986**, *137B*, 320.
- Wignall, G. D.; Bates, F. S. *J. Appl. Crystallogr.* **1986**, *20*, 28.
- Hayashi, H.; Flory, P. J.; Wignall, G. D. *Macromolecules* **1983**, *16*, 1328.
- Hadziioannou, G.; Stein, R. S. *Macromolecules* **1984**, *17*, 567. Stein, R. S.; Hadziioannou, G. *Macromolecules* **1984**, *17*, 1059.
- Warner, M.; Higgins, J. S.; Carter, A. J. *Macromolecules* **1983**, *16*, 1931.
- de Gennes, P.-G. In *Scaling Concepts in Polymer Physics*; Cornell University Press: Ithaca, NY, 1979; Chapter 5.
- Wignall, G. D. *Encyclopedia of Polymer Science and Engineering*; Grayson, M., Kroschwitz, E. M., Eds.; John Wiley and Sons: New York, 1987; Vol. 10, p 112.
- Boué, F.; Nierlich, M.; Leibler, L. *Polymer* **1982**, *23*, 29.
- Nicholson, J. C.; Finerman, T.; Crist, B. *Polymer* **1990**, *31*, 2287.
- Rhee, J.; Crist, B. C. *Macromolecules* **1991**, *24*, 5665.
- Rhee, J.; Crist, B. C. *Macromolecules* **1993**, *98*, 4174.
- Graessley, W. W.; Krishnamoorti, R.; Balsara, N. P.; Fetters, L. J.; Lohse, D. J.; Schultz, D. N.; Sissano, J. A. *Macromolecules* **1993**, *26*, 1137.
- Cassassa, E. F.; Berry, G. C. *J. Polym. Sci., Polym. Phys. Ed.* **1966**, *4*, 881.
- Debye, P.; Bueche, A. M. *J. Appl. Phys.* **1949**, *20*, 518. Debye, P.; Anderson, H. R.; Brumberger, H. *J. Appl. Phys.* **1957**, *28*, 679.
- Fernandez, A. M.; Wignall, G. D.; Sperling, L. H. *Adv. Chem. Ser.* **1986**, *211*, 153.
- Wignall, G. D.; Lin, J. S.; Spooner, S. *J. Appl. Crystallogr.* **1990**, *23*, 241.
- Wignall, G. D. *J. Appl. Crystallogr.* **1991**, *24*, 479.
- Lohse, D. *J. Polym. News* **1986**, *12*, 8.
- Westerman, L.; Clark, J. C. *J. Polym. Sci. Polym. Phys. Ed.* **1973**, *11*, 559.
- Chung, C.; Clark, J. C.; Westerman, L. In *Advances in Polymer Science and Engineering*; Pae, K. D., Morrow, D. R., Chen, D. R., Eds.; Plenum Press: New York, 1972; p 249.